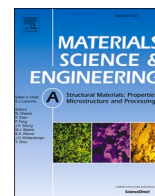




Contents lists available at ScienceDirect

Materials Science & Engineering A

journal homepage: <http://www.elsevier.com/locate/msea>

Short communication

Using high-pressure torsion to fabricate an Al–Ti hybrid system with exceptional mechanical properties

Aleksandra Bartkowska^a, Piotr Bazarnik^{a,*}, Yi Huang^{b,c}, Malgorzata Lewandowska^a, Terence G. Langdon^c^a Warsaw University of Technology, Faculty of Materials Science and Engineering, Woloska, 141, 02-507, Poland^b Department of Design and Engineering, Faculty of Science and Technology, Bournemouth University, Poole, Dorset, BH12 5BB, UK^c Materials Research Group, Department of Mechanical Engineering, University of Southampton, Southampton, SO17 1BJ, UK

ARTICLE INFO

Keywords:

Aluminium
High-pressure torsion
Hybrid materials
Titanium
Ultrafine grains

ABSTRACT

A novel hybrid material was fabricated from the Al–Ti system using high-pressure torsion up to 50 turns. Microstructural observations revealed intermetallic phases and mixing zones enriched in Ti, consisting of grains of ~20 nm within an Al matrix. Microhardness measurements gave values higher than in the HPT-processed bulk aluminium alloy.

The fabrication of multi-layered hybrid materials is a new concept that may be used to enhance the strength of ultrafine-grained (UFG) materials without losing their ductility. The earliest research was conducted by using high-pressure torsion (HPT) to process semi-circular disks of Ag–Ni [1], Nb–Zr [1] and Al–Cu [2] or quarter disks of Al–Cu [3] where these partial disks were placed to form whole disks within the HPT facility. Later, a new approach was developed by separately stacking disks for HPT processing using Al–Mg [4–7], Cu–Sn [8] and Al–Cu, Al–Fe and to perform some preliminary tests on Al–Ti [9]. The Al–Ti system is especially interesting due to the excellent mechanical properties such as high strength, toughness and stiffness combined with a low density which makes it a good candidate material for use in automotive and aerospace applications [10–12]. Therefore, several attempts have been made to fabricate Al–Ti composites using different techniques such as cold-roll bonding [10,11,13], accumulative roll bonding [14–16], explosive welding [17] and powder consolidation by HPT [18]. The present research was initiated to evaluate the potential for achieving high mechanical properties by processing a stacking of Al/Ti/Al disks by HPT.

The initial disks of 10 mm diameter were cut from a commercial purity aluminium alloy (Al-1050) and titanium (CP–Ti). The initial grain sizes were 44 and 25 μm for these two materials, respectively. The aluminium disks were mechanically polished to a final thickness of ~0.4 mm and titanium to a final thickness of ~0.15 mm. These disks

were then stacked in a sequence of one Ti disk between two Al disks using the procedure described earlier [4,5]. The stacks of three disks were then processed by HPT at room temperature under a pressure of 6.0 GPa for 10, 30 and 50 turns. After every 10 rotations, excepting only after the last 10, a heat treatment was applied consisting of annealing the samples in a furnace for 30 min at 300 °C to soften the Al alloy and allow further deformation. It should be emphasized that the temperature of 300 °C is too low to have any major impact on phase transformations in the Al–Ti system.

After processing, each disk was cut vertically along a diameter to give two semi-circular disks and then examined on the cross-sections using light microscopy (LM) with a Zeiss Axio Observer. Panoramic images were made of the overall cross-sections in order to permit a preliminary examination of the quality of bonding between the individual components. Thereafter, observations were undertaken by scanning electron microscopy (SEM) in back-scatter electron (BSE) mode in the peripheral regions. Detailed microstructural observations were performed using a scanning-transmission electron microscope (STEM) Hitachi HD-2700 operating at an accelerating voltage of 200 kV. Samples for the STEM observations were prepared using a focused ion beam facility (FIB) Hitachi NB5000. X-ray diffraction analysis was undertaken at room temperature to analyse the phase composition of the sample processed by HPT for 50 turns. Diffraction patterns were recorded using a Bruker D8 Advance X-ray diffractometer with filtered radiation of

* Corresponding author.

E-mail address: Piotr.Bazarnik@pw.edu.pl (P. Bazarnik).<https://doi.org/10.1016/j.msea.2020.140114>

Received 17 April 2020; Received in revised form 12 August 2020; Accepted 13 August 2020

Available online 19 August 2020

0921-5093/© 2020 The Authors. Published by Elsevier B.V. This is an open access article under the CC BY license (<http://creativecommons.org/licenses/by/4.0/>).

CuK α . Microhardness measurements were recorded using a Zwick/Roell Z2.5 hardness testing machine with a load of 200 g. Linear analysis was performed on one-half of the cross-section with distances between consecutive measurement points of 0.2 mm. The initial coarse-grained materials and the initial materials after 10 HPT revolutions were used as reference samples.

The LM panoramic images of the Al–Ti composites are presented in Fig. 1 after 10, 30 and 50 turns. In the sample after 10 turns there was no intensive bonding between the components with some delamination in the central regions and the Ti disk was only slightly fragmented, whereas after 30 and 50 turns monolithic samples were obtained without evidence for any pores or defects at the Al/Ti interfaces. It is readily apparent that increasing the numbers of HPT turns produces successive fragmentation of the Ti disk. In the sample after 50 turns, there is a continuous bond between components throughout the cross-section but with a gradient in Ti fragmentation moving away from the edge of the sample where the deformation is the highest. The size of the fragmented Ti increases after 50 turns and reaches a maximum size near the centre of the disk. At the edges of the sample, where the applied strain is the largest at the macroscopic scale, it is hard to distinguish between the Al and Ti phases, thereby confirming a significant mixing between these components.

Fig. 2 shows SEM micrographs of the cross-sections of the Al–Ti hybrid material processed by HPT for 50 turns. The overview image in Fig. 2(a) reveals a homogeneous distribution of Ti in the Al matrix with both Ti-enriched shear bands and fine to relatively large fragments of Ti in the Al. Most of the Ti disk has undergone a severe fragmentation which permits a general mixing between Al and Ti. In this sample, the boundaries between the Al and Ti are not well defined in the mixing zone area and this indicates the possibility of the formation of intermetallic phases (Fig. 2(b)). The character of the Al/Ti interface depends on the distance from the disk centre, with a more complex lamellar structure at the area near the edge of the sample and a flatter Al/Ti interface visible around the central region. A similar structure was noted earlier in HPT-processed Al–Mg [4,9,19] and Al–Cu [2,20,21]. More intense mixing was observed in the edge area which is characterized by a laminated, multi-layered structure. This inhomogeneity is typical for HPT processing as the accumulated strain varies along the radius and reaches a minimum in the central area [22]. It was reported earlier for the Al–Cu [2,20,23] and Al–Mg [4,19] systems that intensive mixing in the edge areas of samples promotes the occurrence of solid-state reactions even at low homologous temperatures. Thus, the present samples contain mixing zones consisting of numerous areas of irregularly-shaped thin layers of Al and Ti and the boundaries between the Al and Ti are no longer distinguishable. A similar observation was reported for the Al–Mg system [19] processed by HPT.

Detailed STEM observations, presented in Fig. 3(a–c), reveal a unique, layered microstructure in which it is possible to differentiate the

Al matrix with an average grain size of ~ 160 nm and an area of mixing, marked in Fig. 3(a and b) with an arrow, that is about 400 nm wide. Those areas of mixing consist of thin layers with very small grains having average sizes of ~ 20 nm, as illustrated in Fig. 3(c) where the interface between the matrix and the mixing zones is free of voids with a homogenous structure in Fig. 3(b). A significant grain refinement, to about 300 nm, is visible in the large Ti-rich particles shown in Fig. 3(d). Fig. 3(e) presents a dark-field image with the corresponding compositional maps for Al and Ti. It is apparent that the measurement area is composed of both Al and Ti and there is a Ti-rich zone in the form of bands located within the Al matrix. The occurrence of significant grain refinement, as well as the presence of both Al and Ti (Fig. 3(d)) and the mixing zones (Fig. 3(a,b,c)), suggests the formation of intermetallic phases from the Al–Ti system and it is important therefore to examine this possibility.

The presence of intermetallic phases was examined using XRD analysis as presented in Fig. 4 where the peaks with high intensity correspond to various crystalline planes of the face-centred cubic (FCC) Al and hexagonal close-packed (HCP) Ti. However, the pattern confirms also the formation of $Ti_{3.3}Al$ and Al_3Ti phases. The fraction of intermetallic phases in the samples after 10 and 30 revolutions was too small for detection. Those intermetallic phases are known for having low density, high hardness, good thermal and oxidation resistance and high melting temperatures and therefore they find applications in the strengthening of Al alloys for high-temperature applications [24,25]. The approach of fabricating Al–Ti metallic composites by stacking disks and using HPT processing was reported earlier but without any evidence for the formation of intermetallic phases [9]. However, the formation of Al_2Ti and Al_3Ti intermetallic phases after processing by HPT was described when processing a mixture of powders where the formation of these intermetallic phases was attributed to short circuit diffusion enhanced by the formation of many defects in the HPT-processed material [18].

Hardness testing was conducted in order to examine the influence of HPT processing and these intermetallic phases on the mechanical properties. The microhardness distributions along the radii are shown in Fig. 5 for measurements taken on the cross-sections of the disks of the Al/Ti/Al systems after processing by HPT for 30 and 50 turns; the microhardness values of the as-received and HPT-processed bulk Al-1050 and CP-Ti are also included for comparison. Thus, the hardness of the hybrid material processed for 50 turns lies between the values of ~ 60 Hv at the disk centre and ~ 300 Hv at the edge of the sample, whereas in samples processed for 30 turns the maximum hardness achieved at the edge was ~ 130 Hv and the hardness in the centre varied around a value of ~ 40 Hv. It is worth noting that for all hybrid samples, the hardness in the central regions is inhomogeneous and exhibits high standard deviations which are associated with the presence of large fragments of undeformed titanium plates. The hardness values of the

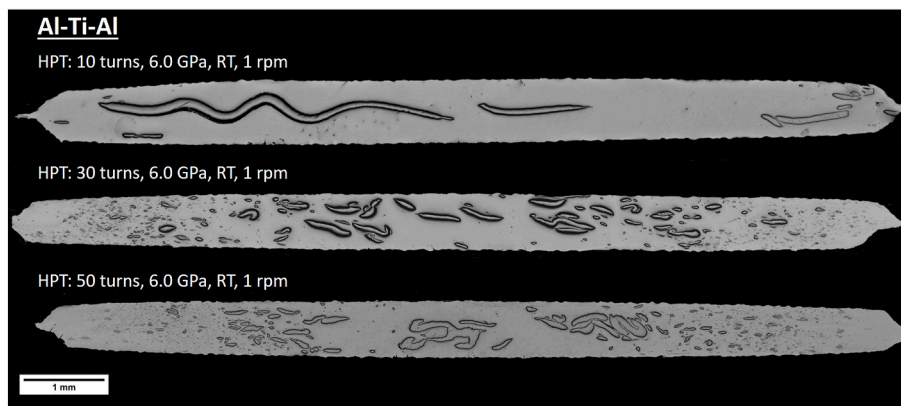


Fig. 1. Vertical cross-sections of the Al–Ti system processed by HPT under an applied pressure of 6.0 GPa for 10, 30 and 50 turns.

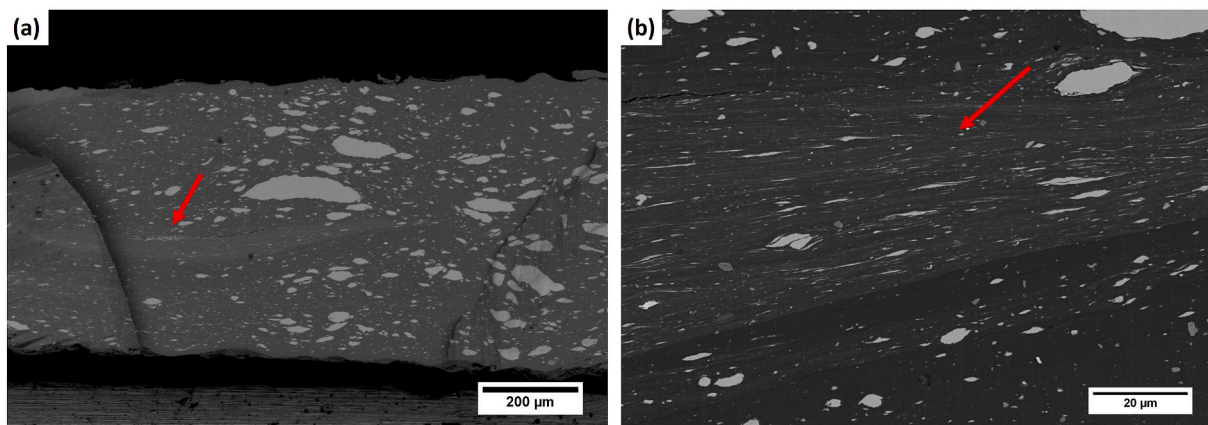


Fig. 2. SEM images of the Al-Ti system processed for 50 turns: (a) overall image of the sample, (b) magnified image of the mixing zones. The brighter contrast corresponds to the Ti-enriched regions and the darker to Al.

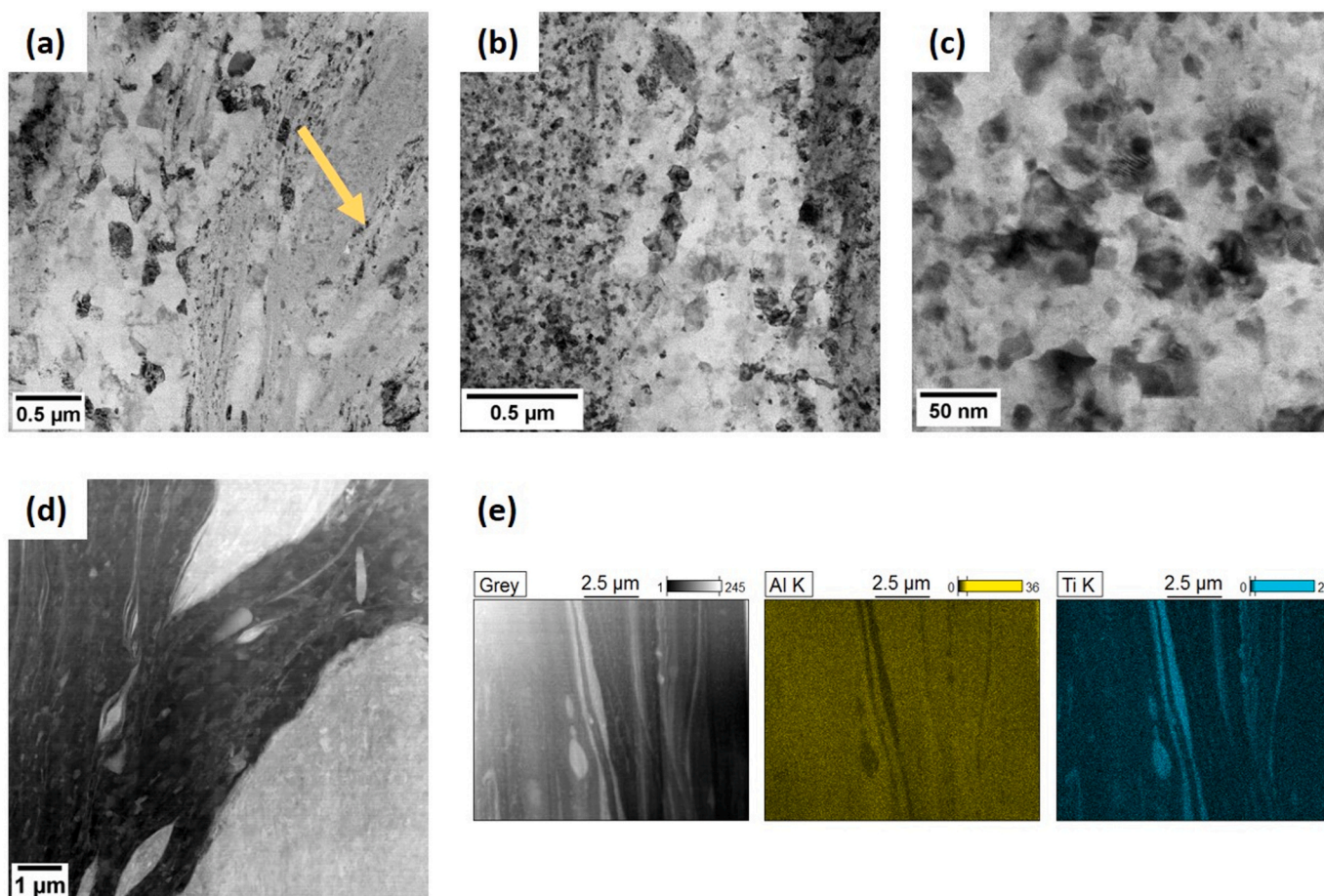


Fig. 3. (a,b) STEM images of the sample of the hybrid material processed for 50 HPT turns, (c) enlarged image of (a), (d) structure of Ti-rich blocks in the Al matrix, (e) EDX compositional maps for Al and Ti containing the mixing zone: dark-field image of the analysed area (left), compositional maps for Al and Ti, in the centre and right, respectively.

hybrid material at the edge are therefore very significantly higher than those for the as-received and HPT-processed Al-1050 and only slightly lower than those for the bulk HPT-processed Ti. It is important to note that the initial system contained 84 vol% of Al and only 16 vol% of Ti so that the hardness of the fabricated hybrid material, which consists mainly of Al, is exceptionally high. This increase in hardness is attributed to Hall-Petch strengthening by grain refinement of the Al matrix and Ti-rich particles and to precipitation hardening due to the formation

of the intermetallic phases [4,19]. A similar increase in hardness was noted for the Al-Mg system where there was a hardness of ~ 270 Hv at the periphery of the sample after processing by HPT for 10 turns [4].

In summary, samples of an Al-Ti hybrid material were fabricated by processing a stack of Al/Ti/Al disks using high-pressure torsion at room temperature for 10, 30 and 50 turns with the application of intermediate appropriate heat treatments. Continuous and complex mixing was observed between Al and Ti after processing by HPT for 50 turns at RT,

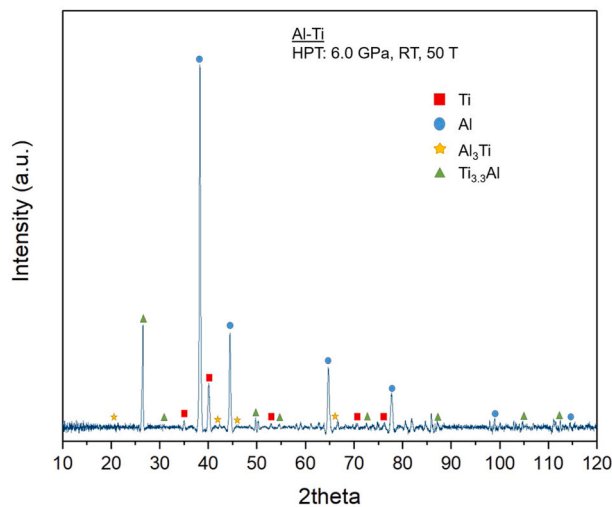


Fig. 4. XRD pattern for the hybrid Al-Ti system processed by HPT for 50 turns.

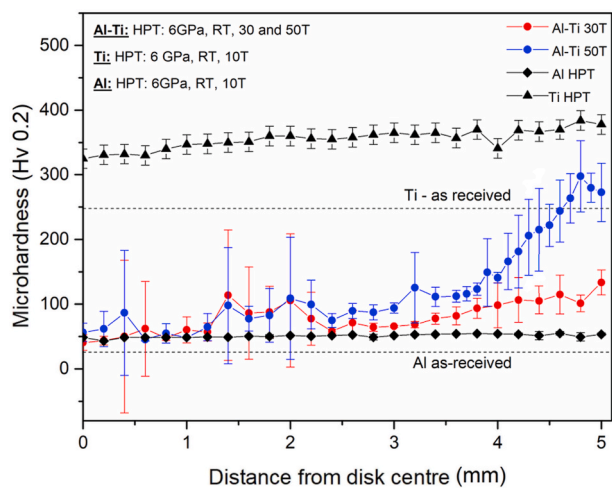


Fig. 5. Microhardness distributions of the hybrid Al-Ti systems processed by HPT for 30 and 50 turns across the half-disk; additional hardness values for the as-received and HPT-processed bulk Al 1050 and Ti are included for comparison.

indicating the potential for using this method as a processing tool for the synthesis of hybrid materials. The microstructure after processing was characterized by exceptional grain refinement, with a grain size of ~ 20 nm inside mixing bands and ~ 160 nm for the Al matrix and ~ 300 nm for Ti-rich blocks. Intermetallic phases from the Al-Ti system were formed during processing by HPT. These phases, together with grain refinement of the Al matrix, the presence of hard Ti-rich blocks and interfaces between the Al and Ti thin layers, lead to a significant increase in the hardness of the hybrid material compared with the hardness of the initial components.

CRedit authorship contribution statement

Aleksandra Bartkowska: SEM studies, Hv measurements. **Piotr Bazarnik:** TEM, FIB, Writing. **Yi Huang:** Visualization, Data processing. **Malgorzata Lewandowska:** Methodology, Data curation, Writing - review & editing. **Terence G. Langdon:** Conceptualization, Supervision, Reviewing and Editing.

Declaration of competing Interest

The authors declare that they have no known competing financial interests or personal relationships that could have appeared to influence the work reported in this paper.

Acknowledgements

This work was supported by the National Science Centre, Poland, within the project SONATINA 1 ‘‘Synthesis of novel hybrid materials using High-Pressure Torsion’’ under Grant Agreement No.2017/24/C/ST8/00145 and by the European Research Council under ERC Grant Agreement No. 267464-SPDMETALS.

References

- [1] T. Miyazaki, D. Terada, Y. Miyajima, C. Suryanarayana, R. Mura, Y. Yokoyama, K. Sugiyama, M. Umamoto, Y. Todaka, N. Tsuji, Synthesis of non-equilibrium phases in immiscible metals mechanically mixed by high pressure torsion, *J. Mater. Sci.* 46 (2011) 4296–4301.
- [2] K. Oh-ishi, K. Edalati, H.S. Kim, K. Hono, Z. Horita, High-pressure torsion for enhanced atomic diffusion and promoting solid-state reactions in the aluminum-copper system, *Acta. Mater.* 61 (2013) 3482–3489.
- [3] O. Bouaziz, H.S. Kim, Y. Estrin, Architecturing of metal-based composites with concurrent nanostructuring: a new paradigm of materials design, *Adv. Eng. Mater.* 15 (2013) 336–340.
- [4] B. Ahn, A.P. Zhilyaev, H.-J. Lee, M. Kawasaki, T.G. Langdon, Rapid synthesis of an extra hard metal matrix nanocomposite at ambient temperature, *Mater. Sci. Eng., A* 635 (2015) 109–117.
- [5] B. Ahn, H.-J. Lee, I.-C. Choi, M. Kawasaki, J.-I. Jang, T.G. Langdon, Micro-mechanical behavior of an exceptionally strong metal matrix nanocomposite processed by high-pressure torsion, *Adv. Eng. Mater.* 18 (2016) 1001–1008.
- [6] M. Kawasaki, B. Ahn, H. Lee, A.P. Zhilyaev, T.G. Langdon, Using high-pressure torsion to process an aluminum-magnesium nanocomposite through diffusion bonding, *J. Mater. Res.* 31 (2016) 88–99.
- [7] J.-K. Han, K.-D. Liss, T.G. Langdon, M. Kawasaki, Synthesis of a bulk nanostructured metastable Al alloy with extreme supersaturation of Mg, *Sci. Rptrs* 9 (2019) 17186.
- [8] A. Korneva, B. Straumal, R. Chulist, A. Kilmametov, P. Bała, G. Cios, N. Schell, P. Zięba, Grain refinement of intermetallic compounds in the Cu-Sn system under high pressure torsion, *Mater. Lett.* 179 (2016) 12–15.
- [9] M. Kawasaki, J.K. Han, D.H. Lee, J.I. Jang, T.G. Langdon, Fabrication of nanocomposites through diffusion bonding under high-pressure torsion, *J. Mater. Res.* 33 (2018) 2700–2710.
- [10] J.G. Luo, V.L. Acoff, Using cold roll bonding and annealing to process Ti/Al multilayered composites from elemental foils, *Mater. Sci. Eng., A* 379 (2004) 164–172.
- [11] J. Peng, Z. Liu, P. Xia, M. Lin, S. Zeng, On the interface and mechanical property of Ti/Al-6%Cu-0.5%Mg-0.4%Ag bimetal composite produced by cold-roll bonding and subsequent annealing treatment, *Mater. Lett.* 74 (2012) 89–92.
- [12] L.M. Peng, J.H. Wang, H. Li, J.H. Zhao, L.H. He, Synthesis and microstructural characterization of Ti-Al3Ti metal-intermetallic laminate (MIL) composites, *Scripta Mater.* 52 (2005) 243–248.
- [13] M. Ma, P. Huo, W.C. Liu, G.J. Wang, D.M. Wang, Microstructure and mechanical properties of Al/Ti/Al laminated composites prepared by roll bonding, *Mater. Sci. Eng., A* 636 (2015) 301–310.
- [14] H.P. Ng, T. Przybilla, C. Schmidt, R. Lapovok, D. Orlov, H.W. Höppel, M. Göken, Asymmetric accumulative roll bonding of aluminium-titanium composite sheets, *Mater. Sci. Eng., A* 576 (2013) 306–315.
- [15] P.D. Motevalli, B. Eghbali, Microstructure and mechanical properties of Tri-metal Al/Ti/Mg laminated composite processed by accumulative roll bonding, *Mater. Sci. Eng., A* 628 (2015) 135–142.
- [16] P. Qu, L. Zhou, V.L. Acoff, Deformation textures of aluminum in a multilayered Ti/Al/Nb composite severely deformed by accumulative roll bonding, *Mater. Char.* 107 (2015) 367–375.
- [17] P. Bazarnik, B. Adamczyk-Cieślak, A. Galka, B. Plonka, L. Sniezek, M. Cantoni, M. Lewandowska, Mechanical and microstructural characteristics of Ti6Al4V/AA2519 and Ti6Al4V/AA1050/AA2519 laminates manufactured by explosive welding, *Mater. Des.* 111 (2016) 146–157.
- [18] Y. Sun, M. Aindow, R.J. Hebert, T.G. Langdon, E.J. Lavernia, High-pressure torsion-induced phase transformations and grain refinement in Al/Ti composites, *J. Mater. Sci.* 52 (2017) 12170–12184.
- [19] J.-K. Han, H.-J. Lee, J. Jang, M. Kawasaki, T.G. Langdon, Micro-mechanical and tribological properties of aluminum-magnesium nanocomposites processed by high-pressure torsion, *Mater. Sci. Eng., A* 684 (2017) 318–327.
- [20] V.N. Danilenko, G.F. Korznikova, A.P. Zhilyaev, S.N. Sergeev, G.R. Khalikova, R. K. Khisamov, K.S. Nazarov, L.U. Kiekukuzhina, R.R. Mulyukov, Effect of annealing on the structure and phase composition of Al-Cu laminated metal-matrix composites produced by shear deformation under pressure, *IOP Conf. Ser. Mater. Sci. Eng.* 447 (2018), 012021. Institute of Physics Publishing.
- [21] G.F. Korznikova, R.R. Mulyukov, A.M. Zhilyaev, V.N. Danilenko, K.R. Khisamov, K. S. Nazarov, S.N. Sergeev, G.R. Khalikova, R.R. Kabirov, Al-Cu layered composites

- fabricated by deformation, AIP Conf. Proc. 2053 (2018), 030028. American Institute of Physics.
- [22] M. Kawasaki, H.-J. Lee, B. Ahn, A.P. Zhilyaev, T.G. Langdon, Evolution of hardness in ultrafine-grained metals processed by high-pressure torsion, *J. Mater. Res. Technol.* 3 (2014) 311–318.
- [23] V.N. Danilenko, S.N. Sergeev, J.A. Baimova, G.F. Korznikova, K.S. Nazarov, R. K. Khisamov, A.M. Glezer, R.R. Mulyukov, An approach for fabrication of Al-Cu composite by high pressure torsion, *Mater. Lett.* 236 (2019) 51–55.
- [24] H.M. Lee, Design of high-temperature high-strength Al-Ti-V-Zr alloys, *Scripta Metall. Mater.* 24 (1990) 2443–2446.
- [25] Y.V. Milman, D.B. Miracle, S.I. Chugunova, I.V. Voskoboinik, N.P. Korzhova, T. N. Legkaya, Y.N. Podrezov, Mechanical behaviour of Al₃Ti intermetallic and L1₂ phases on its basis, *Intermetallics* 9 (2001) 839–845.